Modeling of multichannel filter based on metallo-dielectric nano photonic crystal with coupled defect layers

H. AZARSHAB*, A. GHARAATI
Department of Physics, Payame Noor University, Islamic Republic of Iran

In this paper, we study a multichannel filter by using one dimensional (1D) metallo-dielectric photonic crystal (PC). First, the band gap width (BGW) is examined in normal incidence. Next, we investigate transmission spectra in terms of wavelength for different number of defect layers. Also, we show the influence of different angles of incidence on BGW and wavelength of defect mode in transverse electric (TE) and transverse magnetic (TM) polarizations on the plane of wavelength and incident angle. Then, we demonstrate the effect of different thicknesses of defect layer on transmission spectra. Besides, we investigate transmittance in terms of wavelength and its dependence on the different thickness of dielectric defect layer. Furthermore, we demonstrate that by increasing the number of defect layer and also by increasing thickness of defect layer, the defect mode will be increased. The theoretical analysis shows this structure of combined PC can use as a multichannel filter within a certain wavelength range.

(Received October 2, 2017; accepted February 12, 2019)

Keywords: Multichannel filter, Binary photonic crystal, Metallo-dielectric photonic crystal, Band gap

1. Introduction

An optical filters are devices that selectively transmit light of various wavelengths, while blocking the remainder which is called PBG [1-3]. A metallo-dielectric PC is a periodic structure containing dielectric and metal elements with different refractive indices. There are a lot of advantages to use metals in PCs such as decreased size, simpler fabrication, and lower costs [4]. 1DPCs because of its easy fabrication has many applications such as multilayer's coatings [5], Bragg reflectors [6], and narrow band filters [7, 8]. PBG is in the ranges of frequency in which light cannot propagate through the PC. There are many researches in using dielectric [9, 10], metals [11-14], superconductors and plasmas [15-18], in PCs.

In this paper, we use transfer matrix method (TMM) [19-21] method to calculate BGW. We apply this method to a 1DPC consisting of periodically dielectric-metal materials for both TE and TM waves. The structure of metallo-dielectric PC which is denoted as $air/(AB)^N/air$ where A means the usual air, N is the number of periods and A, B are the refractive indices of metal and dielectric elements, respectively. This structure is depicted in Fig. 1.

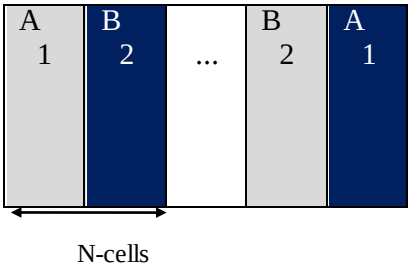

Fig. 1. The structure of metallo-dielectric PCs

2. Theoretical analysis

A Multichannel filter with the structure $air/(AB)^N(ABAC)^M(ABA)(BA)^N/air$ is made of dielectric defect layer (C)with thickness d_d sandwiched by two N-cells in which it puts in air $(n_A = 1)$, and each cell makes up with a dielectric layer A and metallic layer B. The index of refraction of the layers is denoted by n_1 and n_2 respectively, as shown in Fig. 1. The Drude model [22, 23] is invoked to characterize the wavelength dependence of metallic layer.

We have used TMM in our calculations [24]. Each layer of PC has its own transfer matrix and the overall transfer matrix of the system is the product of individual transfer matrices, so the characteristics matrix $M(\Lambda)$ for a single period is expressed as [12, 26- 28]

$$M(\Lambda)=\begin{bmatrix} M_{11} & M_{12} \\ M_{21} & M_{22} \end{bmatrix}=\prod_{\ell=1}^{2}\begin{bmatrix} \cos\beta_\ell & \frac{1}{ip_\ell}\sin\beta_\ell \\ -ip_\ell\sin\beta_\ell & \cos\beta_\ell \end{bmatrix} \quad (1)$$

where $p_\ell = n_\ell\cos\theta_\ell$, $\beta_\ell = k_0 n_\ell d_\ell\cos\theta_\ell$ with $\ell = 1$ and 2. Then, the total characteristic matrix of the total PC is given by [20-24],

$$M_T=\begin{bmatrix} m_{11} & m_{12} \\ m_{21} & m_{22} \end{bmatrix}=(M_1M_2)^N(M_1M_2M_1M_d)^M(M_1M_2M_1)(M_2M_1)^N \quad (2)$$

So the transmission coefficient t is given by

$$t = 2p_0/(m_{11}+m_{12}p_0)p_0+(m_{21}+m_{22})p_0 \quad (3)$$

where $p_0 = n_0\cos\theta_0$. We can calculate the transmittance [23, 28].

$$T = |t|^2 \quad (4)$$

The above calculations can be used for TM wave by substituting $p_\ell = \cos\theta_\ell / n_\ell$ where $\ell = 0$, 1 and 2.

3. Numerical results and discussion

In this work, the layer D means 1 is Si in which refractive index and thickness is $n_1 = 3.45, d_1 = 90nm$. The metallic layer is taken to be silver (Ag) with the plasma frequency $\omega_p = 2\pi\times 2.175\times 10^{15} rad/s$ [29-31] and $d_2 = 10nm$. The substrate is assumed to be air. The number of unit cells is equal to $N = 10$.

3.1. Normal incidence

In Fig. 2, we plot the wavelength dependent transmittance for the metallo-dielectric PC for normal incidence and with the number of unit cells $N = 10$. It is seen that there exists just a PBG.

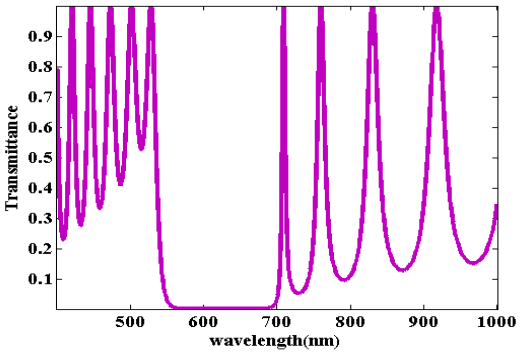

Fig. 2. The calculated wavelength dependent transmittance in metallo-dielectric PC with normal incidence

In Fig. 3, we have plotted the calculated wavelength-dependent transmittance $T(\lambda)$ for the structure $air/(AB)^N(ABAC)^M(ABA)(BA)^N/air$ at different number of defect layers (M) in normal incidence. As we see by increasing *M*, defect modes increase. We give the wavelength of defect modes for different *M* in Table 1.

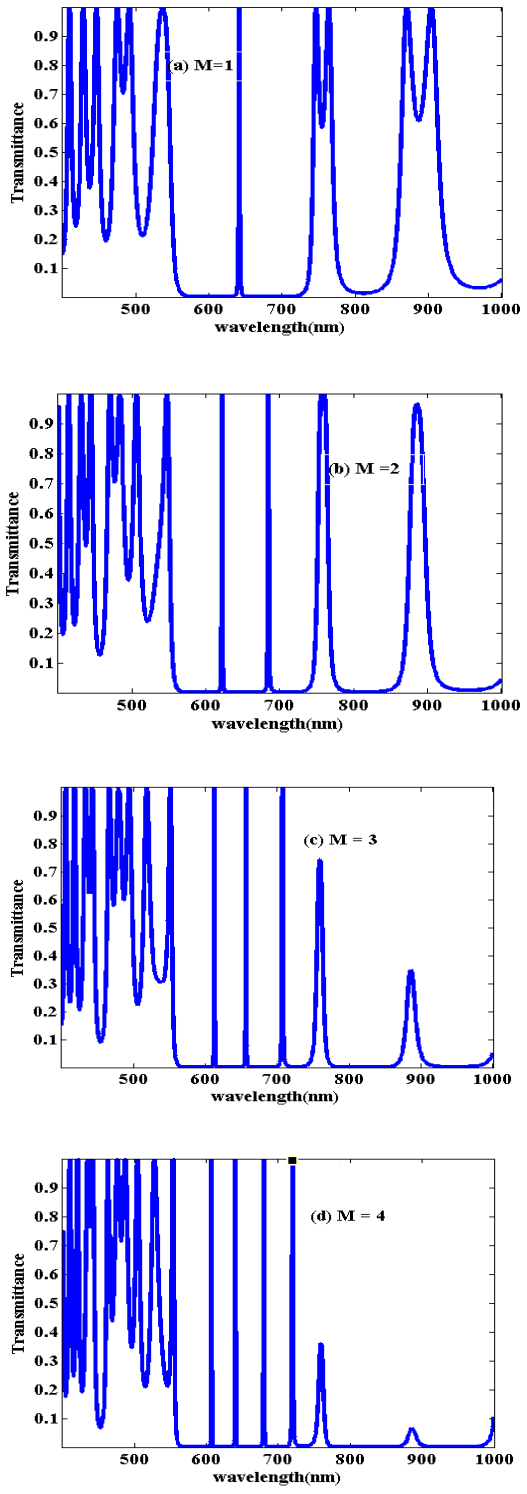

Fig. 3. The calculated wavelength-dependent transmittance in metallo-dielectric PC at M = 1, 2, 3 and 4

Table 1. The number of defect modes and its location for different dielectric defect layers

M	*No.of defect modes*	*wavelength (~nm)*
1	*1*	*639*
2	*2*	*620,684*
3	*3*	*612,656,707*
4	*4*	*607,640,679,719*
5	*5*	*603,630,661,695,727*
6	*6*	*601,623,649,677,706,732*

In Fig. 4, we show the effect of different thicknesses of dielectric defect layer on the transmittance response. We use, N = 4 since defect mode will be appear clearer in it. Besides, according to the constraint $d_{def} = q\lambda_0/4n_d$, where design wavelength $(\lambda_0 = 500nm)$, defect index of refraction $(n_d = 2.13)$ and with different coefficient (q), the thickness will be changed. The number of defect modes is increasing with enhancement of q. We see that by increasing the thickness of defect layer, resonant peak move to the shorter wavelengths. We give the number of defect modes and its location for different thickness of dielectric defect layer by changing q according to the constraint $d_{def} = q\lambda_0/4n_d$ in Table 2.

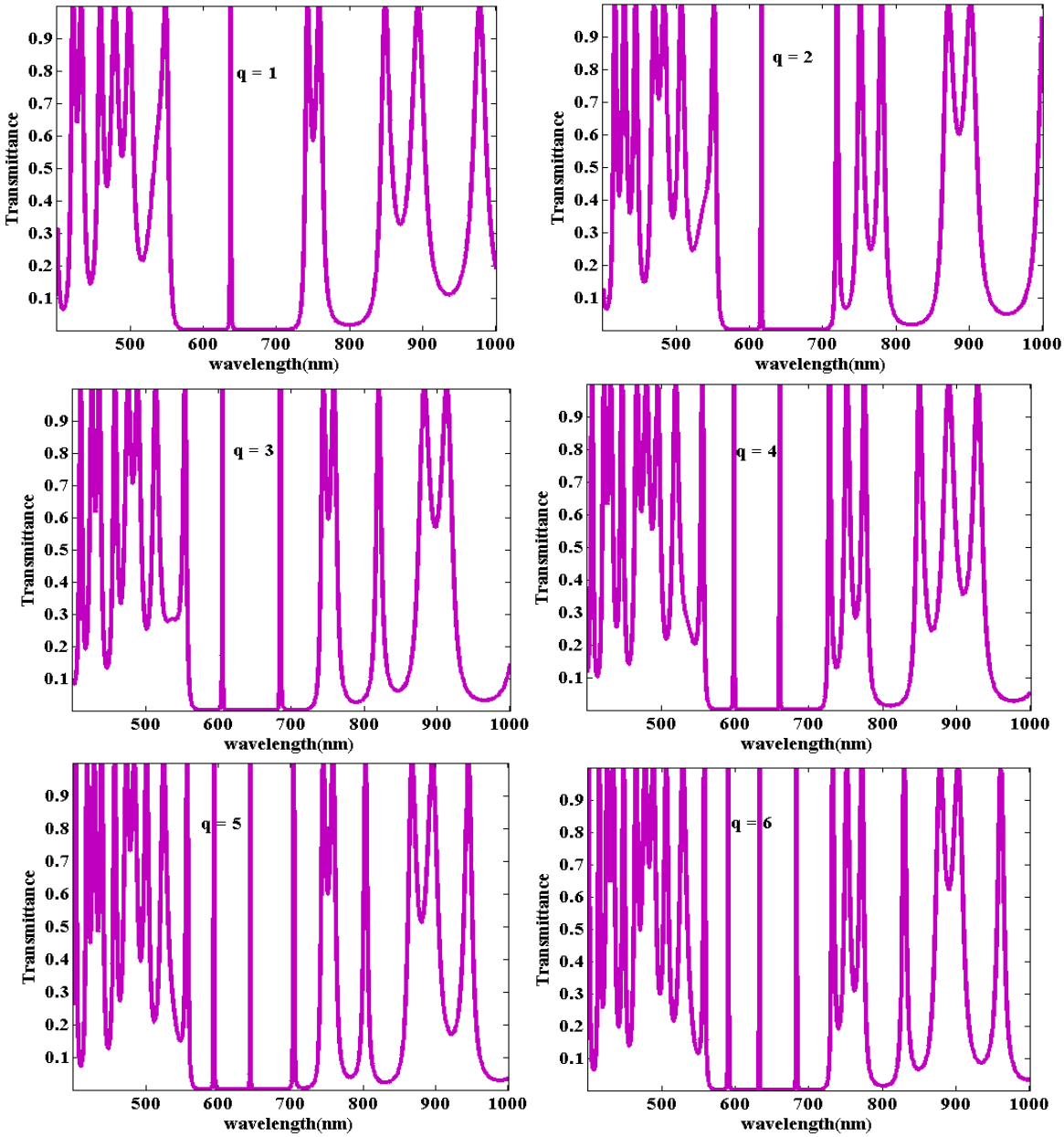

Fig. 4. The wavelength-dependent transmittance for the structure $air/(AB)^N(ABAC)^M(ABA)(BA)^N/air$ *with M=1 and N=4 at different thicknesses of dielectric defect layer by changing q according to the constraint* $d_{def} = q\lambda_0/4n_d$ *from 1 to 6*

Table 2. The number of defect modes and its locations for different thicknesses of dielectric defect layer by changing q according to the formula $d_{def} = q\lambda_0/4n_d$

q	d_{def} (~ nm)	*No. of defect modes*	*Wavelength (~nm)*
1	*58.68*	*1*	*637*
2	*117.37*	*1*	*616*
3	*176.05*	*2*	*605,684*
4	*234.74*	*2*	*598,660*
5	*239.42*	*3*	*593,644,703*
6	*352.11*	*3*	*590,632,683*

3.2. Oblique incidence

In Fig. 5, we plot the transmission response for the structure $air/(AB)^N(ABAC)^M(ABA)(BA)^N/air$ at normal angles of incidence. We know that figures are the same in TE and TM polarizations in the plane of wavelength and angles of incidence for M=0. We see there is just one BG without defect mode in visible region in all angles of incidence. So, for modeling multi channel filter we need to increase M to see defect mode.

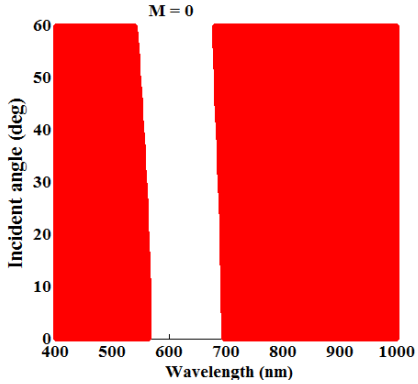

Fig. 5. The calculated wavelength-dependent transmittance for the structure $air/(AB)^N(ABAC)^M(ABA)(BA)^N/air$ *at normal angle of in the plane of wavelength and angles of incidence for M=0*

In Fig. 6, we plot the transmission response for the structure $air/(AB)^N(ABAC)^M(ABA)(BA)^N/air$ at different angles of incidence in TE and TM polarizations in the plane of wavelength and angles of incidence for M=1. We see that by increasing angles of incidence defect modes move to the shorter wavelengths in both TE and TM waves. The BGW does not change by increasing angles of incidence in both TE and TM polarizations. We give the locations of defect modes for different angles of incidence in TE and TM waves with d_d = 120 nm and n_d = 2.13 in Table 3.

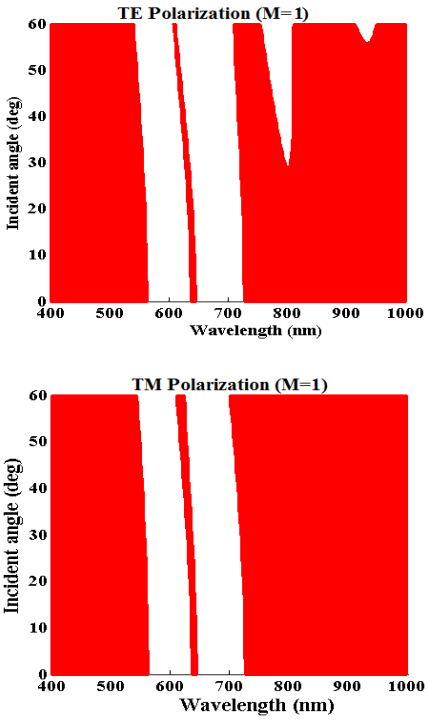

Fig. 6. The calculated wavelength-dependent transmittance for the structure $air/(AB)^N(ABAC)^M(ABA)(BA)^N/air$ *in the plane of wavelength and angles of incidence for M=1 in TE and TM polarizations*

Table 3. The location of defect modes for different angles of incidence in TE and TM waves with d_d = 120 nm *and* n_d = 2.13

angles (degree)	*Defect mode (nm) in TE wave*	*Defect mode (nm) in TM wave*
0	*641*	*641*
10	*639*	*640*
20	*636*	*637*
30	*631*	*633*
40	*624*	*628*
50	*616*	*623*
60	*609*	*618*

In Fig. 7, we show the structure $air/(AB)^N(ABAC)^M(ABA)(BA)^N/air$ at different angles of incidence in TE and TM polarizations for M=2 and M=3. As we observe this structure corresponds to Fig. 3(b) and (c) for TE polarizations and there are two defect modes for M=2 and 3 defect modes for M=3 in both TE and TM polarizations.

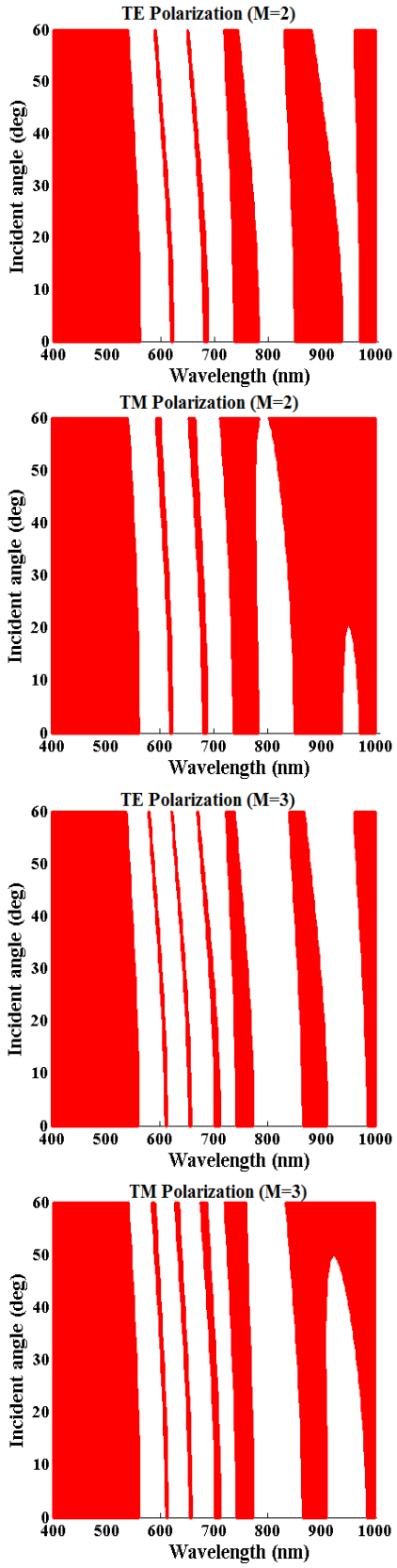

Fig. 7. The calculated wavelength-dependent transmittance for the structure $air/(AB)^N(ABAC)^M(ABA)(BA)^N/air$ *in the plane of wavelength and angles of incidence for M=2 and 3 in TE and TM polarizations*

4. Conclusion

In this paper, we have shown multichannel filter based on defective metallo-dielectric PC with multilayered structure $air/(AB)^N(ABAC)^M(ABA)(BA)^N/air$. We used TMM and the Drude model of metals to calculate PBG and defect modes of this structure. It has been shown that by increasing number of defect layer (M), the defect mode has been increased. Also, we show the influence of different angles of incidence on BGW and wavelength of defect mode in TE and TM polarizations on the plane of wavelength and incident angle and investigate that by increasing angles of incidence, defect mode move to the shorter wavelengths. Besides, we have plotted transmittance in terms of wavelength for different thicknesses of dielectric defect layer and shown that by increasing thickness of defect layer, resonant peaks will be increased. Our analysis shows this structure can be tuned by increasing M, thickness of defect layer and angles of incidence. So it can be used as a multichannel filter within a certain wavelength range.

Acknowledgments

This work has been financially supported by Payame Noor University (PNU) under the Grant of Dr. Gharaati.

References

[1] K. Sakoda, Optical Properties of Photonic Crystals, Springer-Verlag, Berlin, 2001.
[2] M. Skorobogatiy, J. Yang, Fundamentals of Photonic Crystal Guiding, Cambridge University Press, 2009.
[3] J. D. Joannopoulos, R. D. Meade, J. N. Winn, Photonic Crystals: Molding the Flow of Light, Princeton University Press, Princeton, NJ, 1995.
[4] S. Fan, P. R. Villeneuve, J. D. Joannopoulos, Phys. Rev. B **54**, 11245 (1994).
[5] R. Szipocs, K. Ferencz, C. Spielmann, F. Krausz, Optics Letters **19**, 201 (1994).
[6] P. Han, H. Z. Wang, J. Opt. Soc. Am. B **20**, 1996 (2003).
[7] B. A. Usievich, A. M. Prokhorov, V. A. Sychugov, Laser Physics **12**, 898 (2002).
[8] S. K. Awasthi, S. P. Ojha, Progress In Electromagnetics Research M **4**, 117 (2008).
[9] B. Xu, G. Zheng, Y. Wu, Mod. Phys. Lett. B **29**(23), 128 (2015).
[10] H. Azarshab, A. Gharaati, PIER Lett. **71**, 61 (2017).
[11] H. Azarshab, A. Gharaati, Progress In Electromagnetics Research B **37**, 125 (2012).
[12] H. Azarshab, A. Gharaati, PIER Lett. **68**, 113 (2017).
[13] A. Gharaati, H. Azarshab, International Journal of Physics **37**, 149 (2011).
[14] H. Azarshab, A. Gharaati, Microelectronic Engineering **198**, 93 (2018).
[15] S. K. Awasthi, R. Panda, P. K. Chauhan, L.

Shiveshwari, Physics of Plasmas **25**, 052103 (2018).
[16] S. K. Awasthi, R. Panda, L. Shiveshwari, Physics of Plasmas **24**, 072111 (2017).
[17] S. Feng, J. Merle Elson, L. O. Pamela, Optics Express **13**, 4113 (2005).
[18] L. Wei Hsiao, W. Chien-Jang, Y. Tzong-Jer, C. Shoou-Jinn, Optics Express **18**, 27155 (2010).
[19] P. Yeh, Optical Waves in Layered Media, Wiley, New York, 2005.
[20] K. Tang, Y. Xiang, S. Wen, Proc. of SPIE **6020**, 0S.1 (2000).
[21] M. Skorobogatiy, J. Yang, Fundamentals of Photonic Crystal guiding, Cambridge University Press, 2009.
[22] J. D. Jackson, Classical Electrodynamics, Third Edition, California University, 1999.
[23] C. J. Wu, Y. H. Chung, B. J. Syu, Progress In Electromagnetics Research, PIER **102**, 81 (2010).
[24] M. J. P. Loschialpo, J. Schelleng, J. Appl. Phys. **88**, 5785 (2000).
[25] D. M. Topasna, G. A. Topasna, J. Opt. Soc. Am. A, Education and Training in Optics and Photonics (ETOP), July 5, 230 (2009).
[26] S. K. U. Malaviya, S. P. Ojha, J. Opt. Soc. Am. B: Optical Physics **23**, 566 (2006).
[27] M. Born, E. Wolf, Principles of Optics, Cambridge, London, 1999.
[28] B. E. A. Saleh, M. C. Teich, Fundamentals of Photonics, Wiley, New York, 2007.
[29] S. J. Orfanidis, Electromagnetic Waves and Antennas, Rutgers University, 2008.
[30] P. Yeh, Handbook of Optical Constants of Solids, Phys. 98, 1955.
[31] P. Markos, C. M. Soukoulis, Wave Propagation: From Electrons to Photonic Crystals and Left handed Materials, Princeton University Press, New Jersey, 2008.

*Corresponding author: hadis.azarshab@gmail.com